

Category-wise Attack: Transferable Adversarial Examples for Anchor Free Object Detection

Quanyu Liao¹, Xin Wang^{*2}, Bin Kong³, Siwei Lyu⁴, Youbing Yin², Qi Song², and Xi Wu^{†1}

¹Chengdu University of Information Technology

²CuraCloud Corporation

³University of North Carolina at Charlotte

⁴SUNY Albany

Abstract

Deep neural networks have been demonstrated to be vulnerable to adversarial attacks: subtle perturbations can completely change the classification results. Their vulnerability has led to a surge of research in this direction. However, most works dedicated to attacking anchor-based object detection models. In this work, we aim to present an effective and efficient algorithm to generate adversarial examples to attack anchor-free object models based on two approaches. First, we conduct category-wise instead of instance-wise attacks on the object detectors. Second, we leverage the high-level semantic information to generate the adversarial examples. Surprisingly, the generated adversarial examples are not only able to effectively attack the targeted anchor-free object detector but also to be transferred to attack other object detectors, even anchor-based detectors such as Faster R-CNN.

1. Introduction

The development of deep neural networks supports researchers to solve various computer vision problems. However, these deep learning-based algorithms are vulnerable to adversarial attacks [4, 7, 47, 6, 8, 39, 45, 29, 2]: adding some small even imperceptible adversarial noise can make the algorithms fail. The vulnerability of neural networks is observed in many different applications [3, 5, 21, 19, 48, 43, 27, 13, 9], including detection, one of the hotspots in the field of computer vision. Interestingly, one line of research also uses adversarial examples to improve the robustness of neural networks [22, 32, 33, 1, 36] or to help explain some

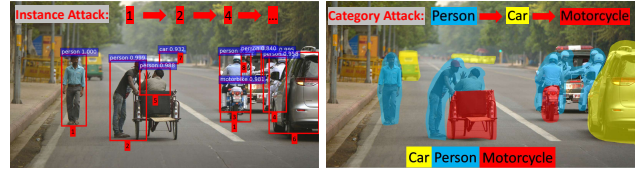


Figure 1. **Left:** Instance-wise attack. The attacker attacks individual objects one by one. **Right:** Our category-wise attack algorithm. The attacker attacks all the objects in a category at the same time.

characteristics of neural network [10].

Regarding the investigation of the vulnerability of deep models in object detection, previous efforts mainly focused on classical anchor-based networks such as Faster-RCNN [38]. However, the performance of anchor-based approaches is limited by the choice of the anchor boxes, and fewer anchor leads to faster speed but lowers accuracy. Thus, advanced anchor-free models such as DenseBox [18], CornerNet [20] and CenterNet [50] are becoming increasingly popular, achieving competitive accuracy with traditional anchor-based models with faster speed and stronger adaptability. However, as far as we know, no existing research has been devoted to the investigation of their vulnerabilities. Adversarial attack methods for Anchor-based [46, 50] are usually not applicable to anchor-free detectors because they generate adversarial examples by selecting the top proposals and attacking them one by one.

To solve these problems, we propose a new algorithm, **Category-wise Attack (CA)**, to attack anchor-free object detection models. It has modules for category-wise attack that jointly attack all the instances in a category (see Fig.1 for details). Unlike most of the existing works [21, 3, 5, 46, 50] which use all the pixels in an anchor proposal for the attack, we select a set of highly informative pixels in the image according to the heatmap which contains higher-level semantic information for the detector. Additionally,

^{*}Corresponding author, xinw@curacloudcorp.com

[†]Corresponding author, xi.wu@cuit.edu.cn

as category-wise attack is challenging, we introduce two Set Attack methods based on two popular adversarial attack techniques, which were originally proposed for attacking image classification models by minimizing the L_0 and L_2 perturbations [28, 14], for attacking object detection models with sparse and dense perturbations, named as Sparse Category-wise Attack (SCA) and Dense Category-wise Attack (DCA) respectively.

To the best of our knowledge, our work is not only the first on attacking anchor-free object detectors but also the first on category-wise attack. We empirically validated our method on two benchmark datasets: PascalVOC [12] and MS-COCO [24]. Experimental results show that our method outperforms the state-of-the-art methods, and the generated adversarial examples achieve superior transferability. To summarize, the contributions of this paper are threefold: **i)** We propose a new method for attacking anchor-free object detection models. Our category-wise attack methods generate more transferable and robust adversarial examples than instance-wise methods with less computational overhead. **ii)** For two widely used L_p norms, *i.e.* L_0 and L_2 , we derive efficient algorithms to generate sparse and dense perturbations. **iii)** Our methods achieve the best transferability performance on two public datasets. Comparing to instance-wise attack methods, our category-wise methods focus on global and high-level semantic information. As a result, they are able to generate more transferable adversarial examples.

2. Related Work

Object Detection. With the fast development of the deep convolutional neural networks, many great solutions have been proposed for object detection. We briefly divide them into anchor-based and anchor-free approaches. Anchor-based object detection models include Faster-RCNN [38], YOLOv2 [37], SSD [25], Mask-RCNN [16], RetinaNet [23]. Compared with anchor-free models, anchor-based object detectors currently achieve relatively higher detection performance.

However, they suffer from two major drawbacks: 1) the network architecture is much more complex and difficult to train, and 2) the anchor scales have to be adjusted to adapt to specific applications, making it difficult to transfer the same network architecture to other dataset/tasks. Recently, anchor-free models like CornerNet [20], ExtremeNet [51] and CenterNet [50] achieve competitive performance with the state-of-the-art anchor-based detectors. These models detect objects by extracting object key-points. In contrast to anchor-based detectors, anchor-free methods are easy to train and free from issues of scale variance.

Adversarial Attack for Image Classification. Goodfellow et al. [15, 42] first showed that deep neural networks are vulnerable to adversarial examples: adding deliberately

generated imperceptible perturbations to the input images can make the deep neural networks output totally wrong results. Since then, a lot of efforts have been devoted to this line of research. To be perceptually imperceptible, most existing adversarial attack algorithms aim to minimize L_p norm of the adversarial perturbations. L_2 and L_∞ norms are two of the most widely used.

Among all the attack algorithms, two most classical ones are FGSM [14] and PGD [26]. The procedure of FGSM is simple. First, the gradient of loss with regard to the input image is computed. Then, the perturbation is assigned with the maximum allowable value in the direction of the gradient. Instead of taking a single large step in FGSM, PGD iteratively takes smaller steps in the direction of the gradient. Compared with FGSM, PGD achieves higher attack performance and generates smaller perturbations. To generate even smaller perturbations, Deepfool was proposed in [30]. It uses the hyperplane to approximate the decision boundary and iteratively computes the lowest euclidean distance between the input image and the hyperplane to generate the perturbations.

However, the above methods suffer from one problem: the generated perturbations are extremely dense—these algorithms have to change almost every pixel of the input image. As a result, the L_0 norm of the perturbation is extremely high. To address this issue, some sparse attack algorithms such as JSMA [35], Sparse Fool, and One-Pixel Attack [41] are proposed to generate sparser perturbations.

Adversarial Attack for Object Detection. The research on the vulnerability of object detection models is scarce. Xie et al. [46] revealed that anchor-based object detection algorithms are hard to resist white-box attacks. UEA [50] leveraged generative adversarial networks (GANs) to improve the transferability of adversarial examples. While DAG and UEA achieved the state-of-the-art attack performance on anchor-based detectors, they suffer from three shortcomings: **(1)** DAG and UEA are based on instance-wise attacks, which only attack one object at a time. As a result, the process is extremely inefficient especially when there exist many objects in the input image. **(2)** UEA relies on a separate GAN network, which needs to be trained each time before being used on a different dataset. Therefore, it is more complex to apply it to a new problem/dataset than optimization-based methods. **(3)** Adversarial examples generated by DAG show poor transferability. While anchor-free object detection models are becoming increasingly popular, no existing research has been devoted to attack these anchor-free detectors. Notably, DAG and UEA can not be applied to attack anchor-free models as they attack detectors by attacking the top proposals and anchor-free detectors do not rely on proposals. Similarly, other anchor proposal-based attackers [21, 3, 5] are also not applicable.

3. Approach

Anchor-free object detectors take as input an image and yield a heatmap for each object category. Then, the object bounding boxes of each category are extracted from the corresponding heatmap with non-maximum suppression. This motivates us to propose category-wise attack instead of instance-wise attack. In this section, we introduce the details of the proposed Category-wise Attack (CA) algorithms. We first formally formulate our category-wise object detection attack problem in Section 3.1. Then, in Section 3.2, we introduce the category-wise target pixel set selection procedure, which is used in both SCA and DCA. Finally, we propose SCA and DCA to generate sparse and dense perturbation respectively in Section 3.3 and 3.4.

3.1. Problem Formulation

The problem of attacking instance-wise object detectors can be formulated as the following objective function:

$$\begin{aligned} & \underset{r}{\text{minimize}} \quad \|r\|_p \\ & \text{s.t.} \quad S(x+r) \cap S(x) = \emptyset \\ & \quad \quad t_{\min} \leq x+r \leq t_{\max} \end{aligned} \quad (1)$$

where x is the original input image. r is the adversarial perturbation. $\|\cdot\|_p$ is the L_p norm, with p possibly be 0, 1, 2, and ∞ . $S(x)$ denotes the object instance set detected by the targeted object detector. $t_{\max}, t_{\min} \in \mathbb{R}^n$ are the maximum and minimum allowable pixel value, which constrains r .

In this paper, we extend the above optimization problem for anchor-free detectors. Suppose there exist K object categories, C_1, C_2, \dots, C_k ($k = 1, 2, \dots, K$). We denote the detected object instances of category C_k on the original input image x as S_k . Then, the objective function becomes:

$$\begin{aligned} & \underset{r}{\text{minimize}} \quad \|r\|_p \\ & \text{s.t.} \quad \forall k, f(x+r, S_k) \notin \{C_1, C_2, \dots, C_K\} \\ & \quad \quad t_{\min} \leq x+r \leq t_{\max} \end{aligned} \quad (2)$$

where $f(x+r, S_k)$ denotes the predicted object categories on the objects set S_k of input image x . Note that it can also be considered as a non-target multi-class attack problem. In this work, we approximate S_k with the heatmap of category C_k generated by CenterNet [50], an anchor-free detector. The details are described in section 3.2.

3.2. Category-wise Target Pixel Set Selection

The attacking procedure of anchor-based attackers is equivalent to using all the available pixels in the bounding box to attack the targeted object instance. Such a mechanism changes a lot of non-informative pixels such as the background pixels, leading to a higher computational overhead as well as adversarial perturbation.

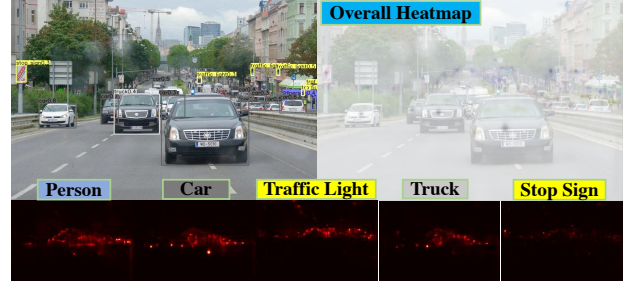


Figure 2. **First row:** Detected results and the overall heatmap of CenterNet [50]. **Second row:** Selected target pixels (Red) for each category.

Instead of attacking all the pixels, we leverage the heatmap, which contains higher-level semantic information for the detectors, to select the target pixel set P . To illustrate this procedure, we use Fig. 2 as an example. Fig. 2 shows the detected results, overall heatmap of the CenterNet [50], and the selected target pixels for each category. In this paper, P is decided by setting an attack threshold. The pixels whose probability score in the heatmap is above the attack threshold are regarded as target pixels and attacked. This strategy helps the attack algorithm to leverage the heatmap to perceive global and higher-level category-wise semantic information, and also reduce the computation time by avoiding attack the instance one by one. We use the target pixel set P as the input for both SCA and DCA.

Algorithm 1 Sparse Category-wise Attack (SCA)

Input: image x , target pixel set P

Output: perturbation r

```

Initialize:  $x^{(0)} \leftarrow x, i \leftarrow 0, j \leftarrow 0, P_{(i)} \leftarrow P$ 
while  $P_i \cap P \neq \emptyset$  do
     $P_{\text{target}, j=0} = \text{SelectPixels}(P_i)$ 
     $x^{(i,0)} \leftarrow x^{(i)}$ 
    while  $j < M$  or  $P_j \cap P_0 \neq \emptyset$  do
         $x_B^{(j)} = \text{DeepFool}(x^{(i,j)})$ 
         $w^{(j)} = \text{ApproxBoundary}(x_B^{(j)}, P_{\text{target}, j})$ 
         $x^{(i,j+1)} = \text{LinearSolver}(x^{(i,j)}, w^{(j)}, x_B^{(j)})$ 
         $P_{\text{target}, j+1} = \text{CheckPixels}(x^{(i,j+1)}, P_{\text{target}, j})$ 
         $j = j + 1$ 
    end while
     $x^{(i+1)} \leftarrow x^{(i,j)}$ 
     $P_{(i+1)} = \text{CheckPixels}(x^{(i+1)}, P_{(i)})$ 
     $i = i + 1, j = 0$ 
end while
return  $r = x^{(i)} - x^{(0)}$ 

```

3.3. Sparse Category-wise Attack

The goal of sparse attack is to make the detectors generate false prediction while perturbing the minimum number of pixels in the input image. This is equivalent to setting $p = 0$ in our optimization problem (2). Sparse Fool [28] was originally proposed to generate sparse perturbations for image classification task. It utilizes linear solver process to achieve lower L_0 perturbations. In this section, we illustrate how to integrate the Sparse Fool method into our anchor-free object detection attacking algorithm, which we term as Sparse Category-wise Attack (SCA) in this paper.

The proposed SCA algorithm is summarized in Algorithm 1. Given an input image x and category-wise target pixels (see 3.2), our algorithm first performs *SelectPixels* to generate the locally target pixel set P_{target} of the target category. In this process, we compute the total probability score of each category and choose the highest one as the target category, then use all detected points which are still not attacked successfully of the target category to construct P_{target} .

Next, we generate sparse perturbation by minimizing $\|r\|_0$ according to P_{target} . Unfortunately, this is an NP-hard problem. We adopt the method employed by DeepFool and Sparse Fool [28] to relax this problem by iteratively approximating the classifier as a local linear function. More specifically, we first generate an initial dense adversarial example x_B with DeepFool [30]. Then, the decision boundary is locally approximated with a hyperplane β passing through x_B :

$$\beta \triangleq \{x : w^T(x - x_B) = 0\} \quad (3)$$

where w is the normal vector of the hyperplane β , which be approximated by the following equation [28]:

$$w := \nabla \sum_{i=1}^n f_{k(x_B, p_i)}(x_B, p_i) - \nabla \sum_{i=1}^n f_{k(x, p_i)}(x_B, p_i) \quad (4)$$

where $f_k(x, p)$ is the k^{th} value of the detection result of heatmap pixel p on input x_B . p_i is the i^{th} pixel of the target pixel set. Then, a sparser adversarial perturbation can be computed by the LinearSolver process [28]. An illustration of this step is given in Fig. 3.

After successfully attacking P_{target} , we use *CheckPixels* to update P_i , which takes as input $x^{(i+1)}$ and P_i . Specifically, we first generate a new heatmap for the perturbed image $x^{(i+1)}$ with the detector. Then, we check whether the confidence of the points on P_i is still higher than the attack threshold on the new heatmap. The points with higher confidence score than the attack threshold is retained, and lower confidence score is retained in P_i , generating a updated target pixel set P_{i+1} . If P_{i+1} is empty, the attack for all object of x is successful and we output the generated adversarial example.

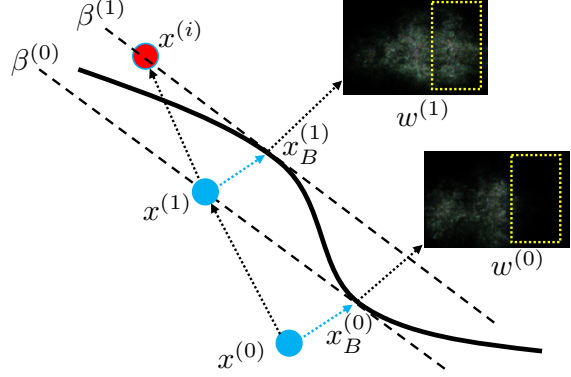


Figure 3. Illustration of SCA, we use the ‘Car’ category in Fig. 2 as an example. The dash lines are the approximated linear decision boundaries in two consecutive iterations. The two images on the right side are the visualization of the normal vector w . We can see that the weights for the ‘Car’ object are reduced (yellow box).

Our algorithm alternates between *SelectPixels* and *CheckPixels*. To immediately remove the successfully attacked pixels, we limit the number of iterations for each P_{target} in the inner loop to M . For example, in Fig. 3, the attack algorithm constructs P_{target} that include the car category. After each iteration, our attack algorithm removes the points which attacked successfully from P and construct new P_{target} . After some iterations, if some pixels with higher w absolute value has been successfully attacked, the points will be removed. Then the remaining points will construct a new P_{target} , and the new P_{target} will generate new w to make sure that the generated adversarial perturbation for the other pixels.

3.4. Dense Category-wise Attack

The goal of dense attack is to make the detectors generate false prediction while minimizing L_∞ of the perturbation. This is equivalent to setting $p = \infty$ in our optimization problem (2). FGSM [14] and PGD [26] are two of the most widely used approaches to attack deep neural networks by minimizing L_∞ . FGSM generates adversarial examples by taking the maximum allowable step in the direction of the gradient of the loss with regard to the input image. Instead of taking a single large step in FGSM, PGD iteratively takes smaller steps in the direction of the gradient. Compared with FGSM, PGD achieves higher attack performance and generates smaller L_∞ perturbations.

Unlike DAG and UEA, which use FGSM to attack object detectors, our adversarial perturbation generation procedure is similar to PGD. In this work, we term our dense attack algorithm as dense category-wise attack (DCA), which is summarized in Algorithm 2. For each iteration i , We generate locally target pixel set P_{target} for each object category k . Different from instance-wise attack algorithms which compute gradients for each single object, we compute gradients for all objects in a category. We compute total loss of P_{target}

Algorithm 2 Dense Category-wise Attack (DCA)**Input:** clean input x , target pixel set P number of class K , perturbation amplitude ϵ' **Output:** perturbation r Initialize: $x^{(0)} \leftarrow x, i \leftarrow 0, k \leftarrow 0, P_i \leftarrow P$ **while** $P_i \cap P \neq \emptyset$ and $i < M_D$ **do** $r_i \leftarrow 0, k \leftarrow 0$ **while** $k < K$ **do** $P_{\text{target}} = \{p_n \mid f(x^{(i)}, p_n) = k, p_n \in P_i\}$ **if** $P_{\text{target}} \neq \emptyset$ **then** $\text{loss}_{\text{sum}} \leftarrow \sum_{p_n \in P_{\text{target}}} \text{CE}(x^{(i)}, p_n)$ $r_k \leftarrow \nabla_{x^{(i)}} \text{loss}_{\text{sum}}$ $r'_k \leftarrow \frac{r_k}{\|r_k\|_\infty}$ $r_i \leftarrow r_i + r'_k$ **end if** $k \leftarrow k + 1$ **end while** $x^{(i+1)} \leftarrow x^{(i)} + \frac{\epsilon'}{M_D} \cdot \text{sign}(r_i)$ $P_{i+1} \leftarrow \text{CheckPixels}(x^{(i+1)}, P_i)$ $i \leftarrow i + 1$ **end while****return** $r = x^{(i)} - x^{(0)}$

of each available category k . Then, we compute adversarial gradient information r_k for each category k and normalize it with L_∞ , yielding perturbation r'_k . Afterward, we add up all r'_k to generate r_i .

Finally, different from DAG which normalize the perturbation with L_∞ , we compute perturbation by applying sign operation to the gradient. sign operation reduces the total number of iterations because L_∞ normalization is not able to generate large enough perturbation in one iteration. As a result, dozens of iterations are required to attack a single object. sign can easily fix this problem. Similar to SCA, we update P_i by *CheckPixels* at the end of each iteration.

4. Experiment

4.1. Experimental Setup

PascalVOC/MS-COCO. We evaluate our method on two popular object detection benchmarks: PascalVOC [12] and MS-COCO [24]. For PascalVOC dataset, we follow previous research [46, 50] to split it to training/testing split: the trainval sets of PascalVOC 2007 and PascalVOC 2012 are used as the training set to train all object detection models, and our adversarial examples are generated on the test set

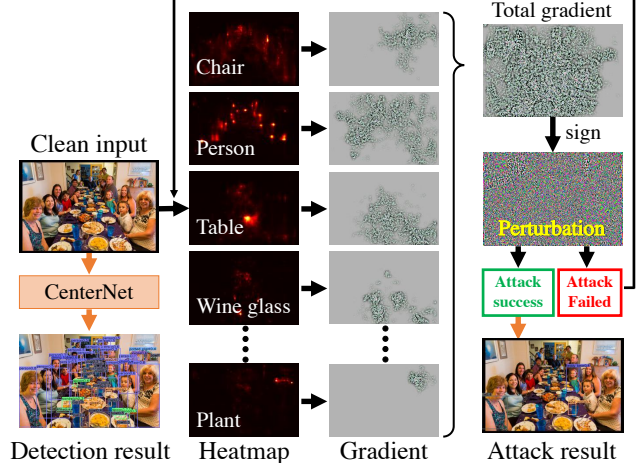


Figure 4. Illustration of DCA. First, we extract the heatmap for each object category and compute gradient information of each object category. After normalizing the adversarial gradients with L_∞ , we add up all gradients and generate adversarial perturbation by further applying sign operation on it. Finally, we check whether the attack is successful. If not, we further generate new perturbation on existing adversarial example in the next iteration.

of PascalVOC 2007, which consists of 4,592 images. Both PascalVOC 2007 and PascalVOC 2012 has 20 categories.

For MS-COCO dataset, we train the object detection models with the training set of MS-COCO 2017 which includes 118,000 images, and the test set consists of 5,000 images. The MS-COCO 2017 dataset contains 80 object categories.

Evaluation Metrics. We use three metrics for the attacking performance of the generated adversarial examples:

i) **Attack Success Rate (ASR):** ASR measures the attack success rate of the generated adversarial examples. It is computed by calculating the mAP (mean Average Precision) loss when substituting the original input images with the generated adversarial examples.

$$ASR = 1 - \frac{mAP_{\text{attack}}}{mAP_{\text{clean}}} \quad (5)$$

where mAP_{attack} denotes the mAP of detector with adversarial example, mAP_{clean} denotes the mAP of clean input.

ii) **Perceptibility:** The goal of attack algorithms is to increase ASR while making the adversarial perturbations not perceptible. We evaluate the perceptibility of adversarial examples by L_2 norm of the adversarial perturbations. Lower L_2 norm indicates lower perceptibility. We evaluate the perceptibility of DCA by $p_{l2} = \sqrt{\frac{1}{k} \sum r_k^2}$, where k is the number of pixels in the image. r_k is normalized in $[0, 1]$. We also evaluate the perceptibility of SCA by P_{l0} , which denotes the proportion of pixels changed after adding the adversarial perturbation.

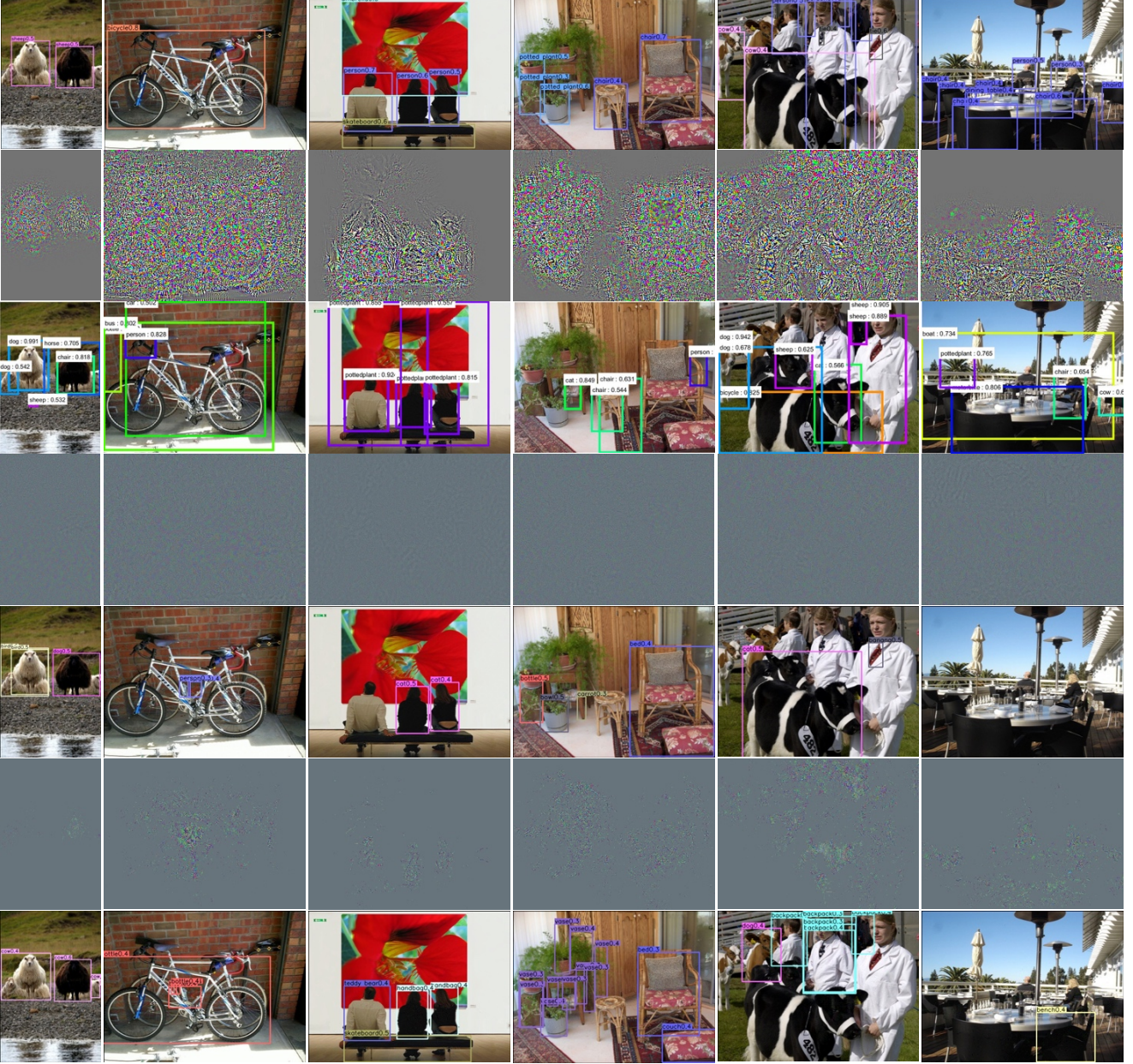


Figure 5. Each column is an example. **Row 1:** Detection results of clean inputs on CenterNet. **Row 2&3:** DAG perturbations and DAG attacked results on Faster-RCNN. **Row 4&5:** DCA perturbations and DCA attacked results on CenterNet. **Row 7&8:** SCA perturbations and SCA attacked results on CenterNet. Note that in **Row 7**, from left to right, the percentage of the changed pixels for each SCA perturbations are: 3.12% 3.4%, 3%, 3.51%, 5.91%, 3.35%. We can see that the perturbations of DCA and SCA are smaller than the DAG’s. Notably, the proposed SCA only changes a few percentage of pixels. To better show the perturbation, we have multiplied the intensity of all perturbation images by 10.

iii) **Attack Transfer Ratio (ATR):** Transferrability is an important property of the adversarial examples [34]. We evaluate the transferrability by computing ATR :

$$ATR = \frac{ASR_{target}}{ASR_{origin}} \quad (6)$$

where ASR_{target} represents the ASR of the attacked target

model and ASR_{origin} denotes the ASR of the model which generate the adversarial example. Higher ATR denotes better transferability.

White-Box/Black-Box Attacks. We conducted both white-box and black-box attacks on several popular object detection models:

From \ To	Resdcn18		DLA34		Resdcn101		CornerNet	
	mAP	ATR	mAP	ATR	mAP	ATR	mAP	ATR
Clean	0.29	–	0.37	–	0.37	–	0.43	–
R18-DCA	0.01	1.00	0.29	0.21	0.28	0.25	0.38	0.12
DLA34-DCA	0.10	0.67	0.01	1.00	0.12	0.69	0.13	0.72
R18-SCA	0.11	1.00	0.27	0.41	0.24	0.57	0.35	0.30
DLA34-SCA	0.07	0.92	0.06	1.00	0.09	0.92	0.12	0.88

Table 1. Black-box attack results on MS-COCO dataset. **From** in the leftmost column denotes the models where adversarial examples generated from. **To** in the top row means the attacked models that adversarial examples transfer to.

From \ To	Resdcn18		DLA34		Resdcn101		Faster-RCNN		SSD300	
	mAP	ATR	mAP	ATR	mAP	ATR	mAP	ATR	mAP	ATR
Clean	0.67	–	0.77	–	0.76	–	0.71	–	0.77	–
DAG [45]	0.65	0.19	0.75	0.16	0.74	0.16	0.60	1.00	0.76	0.08
R18-DCA	0.10	1.00	0.62	0.23	0.65	0.17	0.61	0.17	0.72	0.08
DLA34-DCA	0.50	0.28	0.07	1.00	0.62	0.2	0.53	0.28	0.67	0.14
R18-SCA	0.31	1.00	0.62	0.36	0.61	0.37	0.55	0.42	0.70	0.17
DLA34-SCA	0.42	0.90	0.41	1.00	0.53	0.65	0.44	0.82	0.62	0.42

Table 2. Black-box attack results on PascalVOC dataset. **From** and **To** means the same as Table 1.

	Method	Network	Clean	Attack	ASR (%)	Time (s)
PascalVOC	DAG [46]	FR	0.70	0.050	0.92	9.8
	UEA [44]	FR	0.70	0.050	0.93	–
	SCA	R18	0.67	0.060	0.91	20.1
	SCA	DLA34	0.77	0.110	0.86	91.5
	DCA	R18	0.67	0.070	0.90	0.3
	DCA	DLA34	0.77	0.050	0.94	0.7
MS-COCO	SCA	R18	0.29	0.027	0.91	50.4
	SCA	DLA34	0.37	0.030	0.92	216.0
	DCA	R18	0.29	0.002	0.99	1.5
	DCA	DLA34	0.37	0.002	0.99	2.4

Table 3. Overall white-box performance comparison. The top row denote the metrics. Clean and Attack denotes the mAP of clean input and adversarial examples. Time is the average time to generate the adversarial example.

i) **White-Box Attack:** We conducted attack experiments on two models. Both models use CenterNet but with different backbones: Resdcn18 [17] and DLA34 [49]. We trained these two models on PascalVOC and MS-COCO respectively. We obtain four models from these two backbones and two datasets. We evaluate attack performance of SCA and DCA on each model. In this paper, we denote R18 as CenterNet with Resdcn18 backbone and DLA34 as CenterNet with DLA34 backbone.

ii) **Black-Box Attack:** We classify the black-box attack methods into two categories: cross-backbone and cross-network. In cross-backbone attack, we evaluate the transferability with Resdcn101[17] on PascalVOC and MS-COCO. In the cross-network attack, we use not only anchor-free object detector, but also two-stage anchor-based detectors: CornerNet [20], Faster-RCNN [38] and SSD300 [25]. Faster-RCNN and SSD300 are only tested on PascalVOC.

CornerNet is only tested on the MS-COCO. The backbone is Hourglass [31]. In this paper, we denote FR as Faster-RCNN with VGG16 [40] backbone.

Implementation Details. For both white-box and black-box attacks, we clip the range of the pixel values of the adversarial examples to $[0, 255]$. The attack threshold in Section 3.2 is set to 0.1.

4.2. White-Box Attack Result

We first compare the white-box attack results of our method with the state-of-the-art attack algorithms on PascalVOC. The attack results on CenterNet are summarized in Table 3. From the top half of Table 3, we find that: (1) DCA achieve higher ASR than DAG and UEA and the SCA achieve state-of-art attack performance. (2) DCA is 14 times faster than the DAG. Because UEA is based on GAN, the total attack time should include the training time, but UEA is not open source and we cannot confirm the training time, so we set the attack time of UEA as N/A.

The bottom half of Table 3 shows the attack performance of our methods on MS-COCO. We only compare ASR with DAG and UEA as they didn’t report their performance on MS-COCO. ASR of SCA on two backbones achieve almost the same ASR as the DAG and UEA on PascalVOC: 92.8%, and the ASR of DCA is higher than 99%, meaning that almost all objects can not be detected correctly. It is obvious that both DCA and SCA achieve state-of-the-art attack performance on different models. We also show some qualitative comparison results between DAG and our methods in Fig. 5.

Network	p_{l2}	p_{l0}
DAG	2.8×10^{-3}	$> 99\%$
R18-Pascal	5.1×10^{-3} (DCA)	0.22% (SCA)
DLA34-Pascal	5.1×10^{-3} (DCA)	0.27% (SCA)
R18-COCO	4.8×10^{-3} (DCA)	0.39% (SCA)
DLA34-COCO	5.2×10^{-3} (DCA)	0.65% (SCA)

Table 4. Quantitative perceptibility results of the generated perturbation.

4.3. Black-Box Attack Result/Transferability

To simulate a real-world attack transferring scenario, we use DCA or SCA to generate the adversarial examples on the CenterNet and save them in the JPG format. Saving the adversarial examples in JPG format (JPG compression) may cause them to lose the ability to attack the target models [11] as some key detailed information may be lost during the process. Then, we reload them to attack the target models and compute mAP . This puts a higher demand on the adversarial examples and further guarantees the transferability of the adversarial examples.

Attack transferability on PascalVOC. The adversarial examples are generated on CenterNet with Resdcn18 and DLA34 backbones respectively. We use these adversarial examples to attack other four models. All these five models are trained on the PascalVOC. We can find the DCA is more robust to JPG compression than SCA. But SCA achieves higher ATR than DCA in black-box test. The results are summarized in Table 2, which demonstrate that the generated adversarial examples can successfully transfer to CenterNet with other different backbones, including completely different types of object detectors: Faster-RCNN and SSD.

From Table 2, we also find that DAG is sensitive to JPG compression, especially when the adversarial examples are used to attack Faster-RCNN. And adversarial examples generated by DAG basically lose the ability to attack CenterNet and SSD300. It means both DCA and SCA are better than DAG regarding transferability and the ability to resist JPG compression.

Attack Transferability on MS-COCO. As with PascalVOC, we generate adversarial examples on CenterNet with Resdcn18 and DLA34 backbones and then use them to attack other object detection models. The results are summarized in Table 1. The generated adversarial examples not only can be used to attack other CenterNet with different backbones, but also can be transferred to attack other anchor-free detector: CornerNet. The overall performance on MS-COCO is higher than on PascalVOC. This is because the average mAP of CenterNet on MS-COCO is lower than on PascalVOC. As a result, it makes the confidence of detection accuracies on MS-COCO lower than that on PascalVOC. Lower confidence means that the detector is weaker to defend against the adversarial examples.

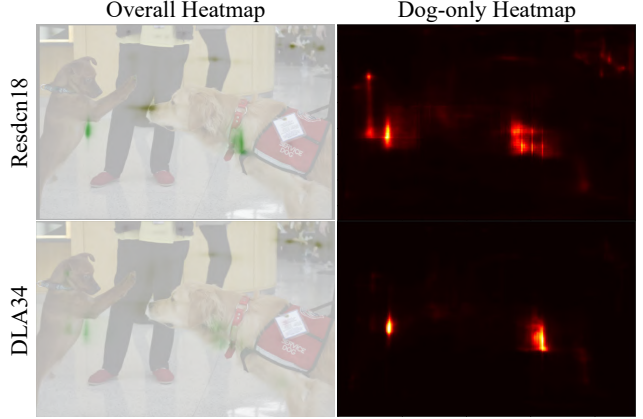


Figure 6. Overall and Dog-only heatmaps generated by DLA34 and Resdcn18. The heatmap from DLA34 is more concentrated on the objects.

The adversarial example are robust to JPG compression on MS-COCO than on PascalVOC.

The adversarial examples generated on DLA34 backbone achieve higher ASR and ATP than backbone Resdcn18, especially on MS-COCO. We also noticed that the adversarial examples generated by models with higher detection performance achieve better attack performance. We guess this is because they produce more accurate heatmaps. To confirm this, we generate heatmaps for a randomly selected image with CenterNet with DLA34 and Resdcn18 backbones (DLA34 achieves better detection performance). The heatmaps of the category dog are shown in Fig. 6. It demonstrates that the heatmap generated by DLA34 are more concentrated on the dogs in the image, while the heatmap predicted by Resdcn18 is more spread out.

4.4. Perceptibility

The perceptibility of the adversarial perturbations of DCA and SCA are shown on Table 4. We evaluate the perceptibility of DCA by p_{l2} and p_{l0} . p_{l0} of SCA is lower than 1%, meaning that SCA can change only a few pixels to fool the detectors. It demonstrates that SCA generates sparse adversarial perturbations. Although the average p_{l2} of DCA is higher than DAG, the perturbations generated by DCA are still hard to be distinguished by human. The p_{l0} of SCA is lower than 1%, meaning that SCA is successful to generate sparse adversarial perturbation. The p_{l0} of DAG and DCA are higher than 99.9%, far more than SCA.

5. Conclusion

In this paper, we propose two category-wise attack algorithms, SCA and DCA, for attacking anchor-free object detectors. Both SCA and DCA focus on global and high-level semantic information to generate adversarial perturbations. SCA is effectively in generating sparse perturbations by generating special decision boundary and approximat-

ing dense adversarial examples. DCA generates perturbations by computing gradients according to global valid categories.

Both SCA and DCA achieve state-of-the-art attack performance in the white-box attack experiments with CenterNet, where DCA is dozens of times faster than DAG and SCA while changing less than 1% pixels. We also test the transferability of DCA and SCA under JPG compression. Both SCA and DCA achieve better attack transferring performance than DAG. The adversarial examples generated by our methods are less sensitive to JPG compression than DAG.

References

- [1] Anish Athalye, Nicholas Carlini, and David Wagner. Obfuscated gradients give a false sense of security: Circumventing defenses to adversarial examples. In *International Conference on Machine Learning (ICML)*, pages 274–283, 2018.
- [2] Shumeet Baluja and Ian Fischer. Adversarial transformation networks: Learning to generate adversarial examples. *arXiv preprint arXiv:1703.09387*, 2017.
- [3] Avishek Joey Bose and Parham Aarabi. Adversarial attacks on face detectors using neural net based constrained optimization. In *IEEE International Workshop on Multimedia Signal Processing (MMSp)*, pages 1–6. IEEE, 2018.
- [4] Nicholas Carlini and David Wagner. Towards evaluating the robustness of neural networks. In *IEEE Symposium on Security and Privacy (SP)*, pages 39–57. IEEE, 2017.
- [5] Shang-Tse Chen, Cory Cornelius, Jason Martin, and Duen Horng Chau. Robust physical adversarial attack on faster r-cnn object detector. *arXiv preprint arXiv:1804.05810*, 2(3):4, 2018.
- [6] Francesco Croce and Matthias Hein. Minimally distorted adversarial examples with a fast adaptive boundary attack. *arXiv preprint arXiv:1907.02044*, 2019.
- [7] Yinpeng Dong, Fangzhou Liao, Tianyu Pang, Hang Su, Jun Zhu, Xiaolin Hu, and Jianguo Li. Boosting adversarial attacks with momentum. In *Proceedings of the IEEE Conference on Computer Vision and Pattern Recognition (CVPR)*, pages 9185–9193, 2018.
- [8] Yinpeng Dong, Tianyu Pang, Hang Su, and Jun Zhu. Evading defenses to transferable adversarial examples by translation-invariant attacks. In *Proceedings of the IEEE Conference on Computer Vision and Pattern Recognition (CVPR)*, pages 4312–4321, 2019.
- [9] Yinpeng Dong, Hang Su, Baoyuan Wu, Zhifeng Li, Wei Liu, Tong Zhang, and Jun Zhu. Efficient decision-based black-box adversarial attacks on face recognition. In *Proceedings of the IEEE Conference on Computer Vision and Pattern Recognition (CVPR)*, pages 7714–7722, 2019.
- [10] Yinpeng Dong, Hang Su, Jun Zhu, and Fan Bao. Towards interpretable deep neural networks by leveraging adversarial examples. *arXiv preprint arXiv:1708.05493*, 2017.
- [11] Gintare Karolina Dziugaite, Zoubin Ghahramani, and Daniel M Roy. A study of the effect of jpg compression on adversarial images. *arXiv preprint arXiv:1608.00853*, 2016.
- [12] Mark Everingham, SM Ali Eslami, Luc Van Gool, Christopher KI Williams, John Winn, and Andrew Zisserman. The pascal visual object classes challenge: A retrospective. *International Journal of Computer Vision (IJCV)*, 111(1):98–136, 2015.
- [13] Kevin Eykholt, Ivan Evtimov, Earlene Fernandes, Bo Li, Amir Rahmati, Chaowei Xiao, Atul Prakash, Tadayoshi Kohno, and Dawn Song. Robust physical-world attacks on deep learning models. *arXiv preprint arXiv:1707.08945*, 2017.
- [14] Ian Goodfellow, Jean Pouget-Abadie, Mehdi Mirza, Bing Xu, David Warde-Farley, Sherjil Ozair, Aaron Courville, and Yoshua Bengio. Generative adversarial nets. In *Advances in Neural Information Processing Systems (NIPS)*, pages 2672–2680, 2014.
- [15] Ian J Goodfellow, Jonathon Shlens, and Christian Szegedy. Explaining and harnessing adversarial examples. *arXiv preprint arXiv:1412.6572*, 2014.
- [16] Kaiming He, Georgia Gkioxari, Piotr Dollár, and Ross Girshick. Mask r-cnn. In *Proceedings of the IEEE Conference on Computer Vision and Pattern Recognition (CVPR)*, pages 2961–2969, 2017.
- [17] Kaiming He, Xiangyu Zhang, Shaoqing Ren, and Jian Sun. Deep residual learning for image recognition. In *Proceedings of the IEEE Conference on Computer Vision and Pattern Recognition (CVPR)*, pages 770–778, 2016.
- [18] Lichao Huang, Yi Yang, Yafeng Deng, and Yinan Yu. Densebox: Unifying landmark localization with end to end object detection. *arXiv preprint arXiv:1509.04874*, 2015.
- [19] Alexey Kurakin, Ian Goodfellow, and Samy Bengio. Adversarial examples in the physical world. *arXiv preprint arXiv:1607.02533*, 2016.
- [20] Hei Law and Jia Deng. Cornernet: Detecting objects as paired keypoints. In *Proceedings of the European Conference on Computer Vision (ECCV)*, pages 734–750, 2018.
- [21] Yuezun Li, Daniel Tian, Xiao Bian, Siwei Lyu, et al. Robust adversarial perturbation on deep proposal-based models. *arXiv preprint arXiv:1809.05962*, 2018.
- [22] Fangzhou Liao, Ming Liang, Yinpeng Dong, Tianyu Pang, Xiaolin Hu, and Jun Zhu. Defense against adversarial attacks using high-level representation guided denoiser. In *Proceedings of the IEEE Conference on Computer Vision and Pattern Recognition (CVPR)*, pages 1778–1787, 2018.
- [23] Tsung-Yi Lin, Priya Goyal, Ross Girshick, Kaiming He, and Piotr Dollár. Focal loss for dense object detection. In *Proceedings of the IEEE Conference on Computer Vision and Pattern Recognition (CVPR)*, pages 2980–2988, 2017.
- [24] Tsung-Yi Lin, Michael Maire, Serge Belongie, James Hays, Pietro Perona, Deva Ramanan, Piotr Dollár, and C Lawrence Zitnick. Microsoft coco: Common objects in context. In *European Conference on Computer Vision (ECCV)*, pages 740–755. Springer, 2014.
- [25] Wei Liu, Dragomir Anguelov, Dumitru Erhan, Christian Szegedy, Scott Reed, Cheng-Yang Fu, and Alexander C Berg. Ssd: Single shot multibox detector. In *European Conference on Computer Vision (ECCV)*, pages 21–37. Springer, 2016.

- [26] Aleksander Madry, Aleksandar Makelov, Ludwig Schmidt, Dimitris Tsipras, and Adrian Vladu. Towards deep learning models resistant to adversarial attacks. *arXiv preprint arXiv:1706.06083*, 2017.
- [27] Jan Hendrik Metzen, Mummadi Chaithanya Kumar, Thomas Brox, and Volker Fischer. Universal adversarial perturbations against semantic image segmentation. In *2017 IEEE International Conference on Computer Vision (ICCV)*, pages 2774–2783. IEEE, 2017.
- [28] Apostolos Modas, Seyed-Mohsen Moosavi-Dezfooli, and Pascal Frossard. Sparsefool: a few pixels make a big difference. In *Proceedings of the IEEE Conference on Computer Vision and Pattern Recognition (CVPR)*, pages 9087–9096, 2019.
- [29] Seyed-Mohsen Moosavi-Dezfooli, Alhussein Fawzi, Omar Fawzi, and Pascal Frossard. Universal adversarial perturbations. In *Proceedings of the IEEE Conference on Computer Vision and Pattern Recognition (CVPR)*, pages 1765–1773, 2017.
- [30] Seyed-Mohsen Moosavi-Dezfooli, Alhussein Fawzi, and Pascal Frossard. Deepfool: a simple and accurate method to fool deep neural networks. In *Proceedings of the IEEE Conference on Computer Vision and Pattern Recognition (CVPR)*, pages 2574–2582, 2016.
- [31] Alejandro Newell, Kaiyu Yang, and Jia Deng. Stacked hourglass networks for human pose estimation. In *European Conference on Computer Vision (ECCV)*, pages 483–499. Springer, 2016.
- [32] Tianyu Pang, Chao Du, Yinpeng Dong, and Jun Zhu. Towards robust detection of adversarial examples. In *Advances in Neural Information Processing Systems (NIPS)*, pages 4579–4589, 2018.
- [33] Tianyu Pang, Kun Xu, Chao Du, Ning Chen, and Jun Zhu. Improving adversarial robustness via promoting ensemble diversity. *arXiv preprint arXiv:1901.08846*, 2019.
- [34] Nicolas Papernot, Patrick McDaniel, Ian Goodfellow, Somesh Jha, Z Berkay Celik, and Ananthram Swami. Practical black-box attacks against machine learning. In *Proceedings of the ACM on Asia Conference on Computer and Communications Security*, pages 506–519. ACM, 2017.
- [35] Nicolas Papernot, Patrick McDaniel, Somesh Jha, Matt Fredrikson, Z Berkay Celik, and Ananthram Swami. The limitations of deep learning in adversarial settings. In *IEEE European Symposium on Security and Privacy (EuroS&P)*, pages 372–387. IEEE, 2016.
- [36] Nicolas Papernot, Patrick McDaniel, Xi Wu, Somesh Jha, and Ananthram Swami. Distillation as a defense to adversarial perturbations against deep neural networks. In *IEEE Symposium on Security and Privacy (SP)*, pages 582–597. IEEE, 2016.
- [37] Joseph Redmon and Ali Farhadi. Yolo9000: better, faster, stronger. In *Proceedings of the IEEE Conference on Computer Vision and Pattern Recognition (CVPR)*, pages 7263–7271, 2017.
- [38] Shaoqing Ren, Kaiming He, Ross Girshick, and Jian Sun. Faster r-cnn: Towards real-time object detection with region proposal networks. In *Advances in Neural Information Processing Systems (NIPS)*, pages 91–99, 2015.
- [39] Yucheng Shi, Siyu Wang, and Yahong Han. Curls & whey: Boosting black-box adversarial attacks. In *Proceedings of the IEEE Conference on Computer Vision and Pattern Recognition (CVPR)*, pages 6519–6527, 2019.
- [40] Karen Simonyan and Andrew Zisserman. Very deep convolutional networks for large-scale image recognition. *International Conference on Learning Representations (ICLR)*, 2014.
- [41] Jiawei Su, Danilo Vasconcellos Vargas, and Kouichi Sakurai. One pixel attack for fooling deep neural networks. *IEEE Transactions on Evolutionary Computation*, 2019.
- [42] Christian Szegedy, Wojciech Zaremba, Ilya Sutskever, Joan Bruna, Dumitru Erhan, Ian Goodfellow, and Rob Fergus. Intriguing properties of neural networks. *arXiv preprint arXiv:1312.6199*, 2013.
- [43] Pedro Tabacof, Julia Tavares, and Eduardo Valle. Adversarial images for variational autoencoders. *arXiv preprint arXiv:1612.00155*, 2016.
- [44] Xingxing Wei, Siyuan Liang, Xiaochun Cao, and Jun Zhu. Transferable adversarial attacks for image and video object detection. *arXiv preprint arXiv:1811.12641*, 2018.
- [45] Chaowei Xiao, Bo Li, Jun-Yan Zhu, Warren He, Mingyan Liu, and Dawn Song. Generating adversarial examples with adversarial networks. In *Proceedings of the International Joint Conference on Artificial Intelligence (IJCAI)*, pages 3905–3911. AAAI Press, 2018.
- [46] Cihang Xie, Jianyu Wang, Zhishuai Zhang, Yuyin Zhou, Lingxi Xie, and Alan Yuille. Adversarial examples for semantic segmentation and object detection. In *Proceedings of the IEEE International Conference on Computer Vision (ICCV)*, pages 1369–1378, 2017.
- [47] Cihang Xie, Zhishuai Zhang, Yuyin Zhou, Song Bai, Jianyu Wang, Zhou Ren, and Alan L Yuille. Improving transferability of adversarial examples with input diversity. In *Proceedings of the IEEE Conference on Computer Vision and Pattern Recognition (CVPR)*, pages 2730–2739, 2019.
- [48] Dawei Yang, Chaowei Xiao, Bo Li, Jia Deng, and Mingyan Liu. Realistic adversarial examples in 3d meshes. *arXiv preprint arXiv:1810.05206*, 2, 2018.
- [49] Fisher Yu, Dequan Wang, Evan Shelhamer, and Trevor Darrell. Deep layer aggregation. In *Proceedings of the IEEE Conference on Computer Vision and Pattern Recognition (CVPR)*, pages 2403–2412, 2018.
- [50] Xingyi Zhou, Dequan Wang, and Philipp Krähenbühl. Objects as points. *arXiv preprint arXiv:1904.07850*, 2019.
- [51] Xingyi Zhou, Jiacheng Zhuo, and Philipp Krahenbuhl. Bottom-up object detection by grouping extreme and center points. In *Proceedings of the IEEE Conference on Computer Vision and Pattern Recognition (CVPR)*, pages 850–859, 2019.